



Simulating the effect of subsurface drainage on the thermal regime and ground ice in blocky terrain, Norway

Cas Renette¹, Kristoffer Aalstad¹, Juditha Aga¹, Robin Benjamin Zweigel^{1,2}, Bernd Etzelmüller¹, Karianne Staalesen Lilleøren¹, Ketil Isaksen³, Sebastian Westermann¹

5

¹Department of Geosciences, University of Oslo, Oslo, Norway

²Centre for Biogeochemistry of the Anthropocene, UiO, Oslo

³Norwegian Meteorological Institute, Oslo, Norway

Correspondence to: Cas Renette (cas.renette@gmail.com)

10 **Abstract.** Ground temperatures in coarse, blocky deposits such as mountain blockfields and rock glaciers have long been observed to be lower in comparison with other (sub)surface material. One of the reasons for this negative temperature anomaly is the lower soil moisture content in blocky terrain, which decreases the duration of the zero curtain in autumn. Here we used the CryoGrid community model to simulate the effect of drainage in blocky terrain permafrost at two sites in Norway. The model setup features a surface energy balance, heat conduction and advection, as well as a bucket water scheme with adjustable lateral drainage. We used three idealized subsurface stratigraphies, denoted *blocks only*, *blocks with sediment* and *sediment only* and are either *drained* or *undrained* of water, resulting in six ‘scenarios’. The main difference between the three stratigraphies is their ability to retain water against drainage: while the *blocks only* stratigraphy can only hold small amounts of water, much more water is retained within the sediment phase of the two other stratigraphies, which critically modifies the freeze-thaw behaviour.

20 The simulation results show markedly lower ground temperatures in the *blocks only, drained* scenario compared to other scenarios, with negative thermal anomaly of up to 1.8–2.2 °C. For this scenario, the model can in particular simulate the time evolution of ground ice, with build-up during and after snow melt and spring and gradual lowering of the ice table in the course of the summer season. We simulate stable permafrost conditions at the location of a rock glacier in northern Norway with a mean annual ground surface temperature of 2.0–2.5 °C in the *blocks only, drained* simulations. Finally, transient simulations at the rock glacier site showed a complete or partial lowering of the ground ice table since 1951 for all simulations except the *blocks only, drained* run.

30 The interplay between the subsurface water/ice balance and ground freezing/thawing driven by heat conduction can at least partly explain the occurrence of permafrost in coarse blocky terrain below the assumed elevational limit of permafrost. It is thus important to consider this effect in future efforts on permafrost distribution mapping in mountainous areas. Furthermore, an accurate prediction of the evolution of the ground ice table in a future climate can have implications for slope stability, as well as water resources in arid environments.



1 Introduction

Permafrost is defined as ground that remains at or below 0 °C for two or more consecutive years (Van Everdingen, 1998) and is a common feature in mountain environments. In discontinuous mountain permafrost terrain, the lowest-lying active
35 permafrost landforms are frequently found in coarse, blocky terrain (Harris and Pedersen, 1998). In particular, rock glaciers are frequently found below the assumed elevational limit of permafrost (Lilleøren and Etzelmüller 2011).

The occurrence of a negative temperature anomaly in coarse, blocky deposits has long been recognized, e.g. in central eastern Norway by Liestøl (1966). Harris and Pedersen (1998) found a negative temperature anomaly of 4 to 7 °C in blocky
40 terrain relative to adjacent mineral sediment in mountains in Canada and China. They summarized four hypotheses that explain these anomalies: (a) The Balch effect; (b) chimney effect; (c) evaporation of water and sublimation of ice in the summer and (d) continuous air exchange with the atmosphere when no continuous winter snow cover is present.

Juliussen and Humlum (2008) showed that block fields in the Norwegian mountains featured a negative temperature anomaly of 1.3 to 2.0 °C, which was mainly attributed to rocks protruding into and through the snow cover which leads to a
45 higher effective thermal conductivity of the snow cover. Gruber and Hoelzle (2008) presented a simple model for the conductive effect of blocks protruding through the snow cover which showed that the mean annual ground temperature is reduced as a result of a lower thermal conductivity of a blocky layer.

Additionally, a lower soil moisture content in permeable blocky debris decreases the duration of the zero-curtain in autumn since less latent heat is liberated compared to soil with higher soil moisture content (Juliussen and Humlum 2008). In
50 spring, the opposite effect is observed when percolating meltwater refreezes at the bottom of the blocky surface layer and confines temperatures at the ice interface to 0 °C (e.g. Juliussen and Humlum, 2008; Hanson and Hoelzle, 2004; Humlum, 1997).

Rock glaciers play an important role in the hydrological cycle, especially in arid regions like the Andes, where in some areas more water is stored in rock glaciers than in glaciers (Jones et al., 2019; Azócar and Brenning, 2010). The open debris structure can act as a trap for snow and a rock glacier can store a significant quantity of ice or liquid water. Rock glaciers
55 studied in Argentina are an important water resource as they release water mainly during periods of drought (Croce and Milana 2002). Ground ice melt as a response to climate warming threatens this water source. Additionally, melting of ground ice can lead to slope instability (e.g. Gruber and Haeberli, 2007; Saemundsson et al. 2018; Nelson et al., 2001) and damage to infrastructure (e.g. Arenson et al., 2009).

In southern Norway, permafrost underlies large parts of areas above 1500 m.a.s.l.. The permafrost elevation limit
60 decreases from above 1600 m.a.s.l. in the west to about 1100 m.a.s.l. in the eastern, more continental areas (Etzelmüller et al., 2003). In northern Norway, the limit is around 800–1000 m.a.s.l. in the west and decreases towards the east. A first inventory of Norwegian rock glaciers based on aerial imagery was published in 2011 (Lilleøren and Etzelmüller, 2011), suggesting that found active permafrost landforms occur above 400 m.a.s.l.. The density of rock glaciers in Norway is lower than in other mountain permafrost areas which was attributed to a lack of bedrock competence and debris availability as well as to the



65 relative lack of steep topography above the permafrost limit. Recently, Lilleøren et al. (2022) described rock glaciers near sea
level in the area of Hopsfjorden, northern Norway, which feature a limited ice body and are in transition from active to relict.
Additionally, Nesje et al. (2022) presented new evidence for active rock glaciers in southern Norway well below the assumed
permafrost limit. Warming of Norwegian mountain permafrost (Etzelmüller et al., 2020) is expected to continue in the 21st
70 century (Hipp et al., 2012), resulting in further degradation of these ice bodies and an upward shift of the lower permafrost
limit. Hipp et al. (2012) also mentioned the need to address the effect of snow cover and surface material on how ground
temperatures respond to climate forcing.

Land surface models that can represent permafrost are vital tools to investigate the sensitivity to climate change and
complex environmental conditions. Since permafrost presence is often not visible at the surface, numerical modelling based
on process understanding is often used to estimate the permafrost distribution (Harris et al. 2009). One-dimensional heat flow
75 models have been used in studies to investigate the effect of climate change on permafrost (e.g. Etzelmüller et al., 2011; Hipp
et al., 2012) or to model specific processes in mountain permafrost (e.g. Gruber and Hoeszle, 2008). However, many such
models do not include a transient representation of the subsurface water and ground ice balance (e.g. Etzelmüller et al., 2011;
Hipp et al., 2012; Westermann et al., 2013).

The CryoGrid community model (Westermann et al., 2022) is a simulation toolbox that can calculate ground
80 temperatures and volumetric water as well as ice content in permafrost environments. It largely builds on the well-established
CryoGrid 3 model (e.g. Westermann et al., 2016; Martin et al., 2019) and accommodates a broad range of applications. In the
following, the CryoGrid community model is referred to as “CryoGrid” for simplicity.

In this study, we present simulations of ground temperatures and ice content for different idealized subsurface
stratigraphies and drainage regimes using CryoGrid, applied at two Norwegian permafrost sites: a blockfield site in southern
85 Norway and a rock glacier in northern Norway. The aim is to contribute to an improved process understanding of the coupled
subsurface energy and water/ice balance, focusing on the observed negative thermal anomaly in coarse, blocky deposits. In
particular, we present simulations how the ground ice mass balance in blocky terrain can affect ground temperatures and the
occurrence of permafrost.

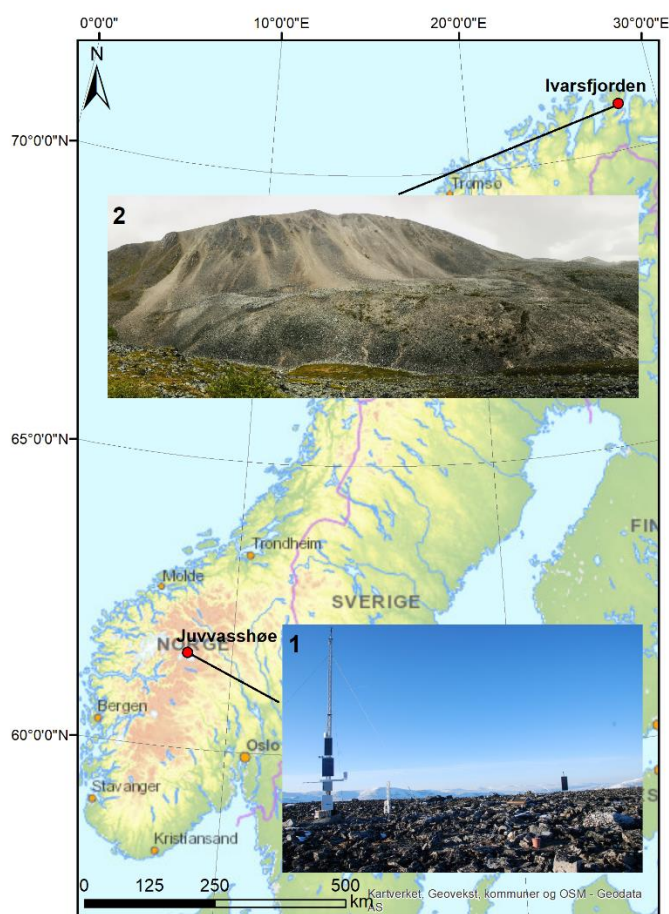
2 Study sites

90 2.1 Juvvasshøe, southern Norway

Juvvasshøe (61°40 N, 08°22 E, 1894 m.a.s.l.) (Fig. 1) is a site located in the southern Norwegian mountains, Jotunheimen well
above the tree line. A 129 m deep borehole was drilled in August 1999 in the PACE (Permafrost and Climate in Europe)
project (Harris et al., 2001). Continuous data streams from this PACE borehole are available with the exception of a gap
between 21 December 2011 to 24 April 2014. The site is located in an extensive block field on a mountain plateau with sparse
95 vegetation cover. The bedrock (crystalline rocks, Farbrot et al., 2011) is located at approximately 5 m depth, the first meter
consists of large stones and boulders and the ground below mainly consists of cobbles (Isaksen et al., 2003). Between 2000



and 2004, Isaksen et al. (2007) measured a mean annual air temperature (MAAT) at 2 m height of $-3.3\text{ }^{\circ}\text{C}$. The mean ground temperature (MGT) at 2.5 m below the surface during this period was $-2.5\text{ }^{\circ}\text{C}$. The mean precipitation was estimated to be between 800 and 1000 mm yr^{-1} . The site is extremely wind-exposed, resulting in a low snow thickness due to wind drift. Hipp et al. (2012) described a snow depth of less than 20 cm, while the snow thickness in surrounding, lower-lying and less exposed sites can be up to 140 cm. Isaksen et al. (2007) measured the difference between the MAGST and MAAT (surface offset) at exposed and less exposed sites in this area. At sites with a significant snow cover, the surface offset was more than $2\text{ }^{\circ}\text{C}$, while at exposed (including Juvvasshøe) sites this offset is generally below $1\text{ }^{\circ}\text{C}$. The permafrost thickness at the PACE borehole was estimated to be approximately 380 m (Isaksen et al., 2001), with the lower permafrost limited at ca. 1450 m.a.s.l. (Farbrot et al., 2011). A weak zero curtain effect suggests a low water content in the active layer (Isaksen et al., 2007). A warming of $0.2\text{ }^{\circ}\text{C}$ per decade and $0.7\text{ }^{\circ}\text{C}$ per decade in surface air temperature and ground surface temperature, respectively, occurred between 2000 and 2019 (Etzelmüller et al., 2020).



110 **Figure 1: Location of the two sites in Norway (© Norwegian Mapping Authority). (1) blockfield at Juvvasshøe (1894 m.a.s.l.), (2) rock glacier at Ivarsfjorden (60–160 m.a.s.l.).**



2.2 Ivarsfjorden rock glacier, northern Norway

Ivarsfjorden is a small fjord arm of the larger Hopsfjorden, located on the Nordkinn peninsula in the Troms and Finnmark county in northern Norway (Fig. 1). Deglaciated around 14–15 cal kyr BP (Romundset et al., 2011), the peninsula is dominated by flat mountain plateaus of exposed bedrock, *in situ* weathered material and coarse grained till (Lilleøren et al., 2022), which feature steep slopes towards the sea. The coastal areas of Finnmark have a wet maritime climate, with mean annual precipitation around 1000 mm (Saloranta, 2012). Lilleøren et al. (2022) describe a MAAT of 1.6 °C between 2010 and 2019 in the area of the rock glacier. The rock glacier of interest lies in a southwest-northeast trending valley that extends from the fjord and has an elevation extent of roughly 60 to 160 m.a.s.l.. The mountain at its east (443 m.a.s.l.) serves as the source area with rockfall debris and coarse talus slopes being common. The bedrock in Ivarsfjorden consists of sandstones and phyllites (NGU, 2008). Sandstones often generate coarse, bouldery material, which is favorable for the formation of rock glaciers (Haeberli et al. 2006). The rock glacier in Ivarsfjorden is northwest facing and has previously been interpreted as relict (Lilleøren and Etzelmüller, 2011), but a detailed analysis showed that a limited ice core might still be present (Lilleøren et al., 2022). A negative MAAT around 100 to 150 years ago is an indication that rock glaciers in this area were active at the end of the Little Ice Age (LIA). Refraction Seismic Tomography (RST) surveys indicate a porous air-filled stratigraphy such as blocky talus deposits. While observed MAGSTs between 2015 and 2020 are all positive, negative surface temperatures during summer have been observed by a thermal camera at the front slope of the rock glacier. This is likely an indication of the chimney effect and thus of connected voids that support air flow.

3. Methods

3.1 The CryoGrid community model

CryoGrid is a simulation toolbox for ground thermal simulations that can be applied to a wide range of applications in the terrestrial cryosphere thanks to its modular structure (Westermann et al., 2022). It has mainly been applied in permafrost environments, using heat conduction to simulate ground temperatures transiently. To represent the energy and water cycle of a one-dimensional ground column in the best possible way, CryoGrid allows the user to select different processes representations/parameterizations for different vertical domains. As an example, a fully transient water balance can be used in the near-surface region, while a constant water(ice) content is used in deeper layers. Likewise, different process representations for the seasonal snow cover can be chosen. To define the properties of the subsurface material, a stratigraphy of volumetric mineral, organic, water and ice content must be provided (Westermann et al., 2022).

In the model setup used for this study, the lower boundary condition is provided by a constant geothermal heat flux of 0.05 Wm^{-2} which is a reasonable value for Norway used in previous modeling studies (Westermann et al., 2013). The upper boundary results from solving the full surface energy balance, including both radiative and turbulent heat fluxes, which gives rise to a ground heat flux. In order to solve the surface energy balance, atmospheric forcing data are required (chapter 3.4). A



scheme with heat conduction, following Fourier's law for heat conduction, and heat advection is used for heat transfer and temperature calculation in the subsurface (Westermann et al., 2022).

145 For soil hydrology, a gravity driven bucket scheme is used. Rainfall is taken from the forcing data and added to the uppermost cell of the subsurface. The surface energy balance calculations determine how the soil moisture is affected by evaporation. Transpiration plays no part in this study as no vegetated surfaces are involved. Water that is in excess of the field capacity infiltrates downwards until either the water table or a frozen cell is reached. The water table forms if excess water is available and cells are saturated from the bottom upwards. If all grid cells are saturated, excess water is considered as surface runoff.

150 The freezing characteristic of water in the subsurface can be set to follow a freeze curve depending on the soil type, following Painter and Karra (2014) or set as free water (water changes state at 0 °C, Westermann et al., 2022) for subsurface material with large pores/voids, such as blocky terrain.

155 Studies that used a previous model version of CryoGrid (e.g. Westermann et al., 2013; Westermann et al., 2016; Langer et al., 2016) assumed constant water/ice contents. This is a major limitation, as varying soil moisture contents strongly affect the ground thermal regime (e.g. Martin et al., 2019). We use a one-dimensional model setup and simulate lateral drainage out of the model domain by assuming a seepage face at atmospheric pressure. First, the elevation of the water table is calculated, after which a lateral water flux removes water in grid cells that are below this water table, following Eq. (1):

$$F_i^{lat} = -K_H \frac{z_{wt} - z_i}{d^{lat}}, \quad (1)$$

160 where F_i^{lat} is the lateral water flux out of grid cell i , K_H is the hydraulic conductivity, z_{wt} is the height of the water table, z_i is the height of grid cell i and d^{lat} is the lateral distance to the seepage face. We use the parameter d^{lat} to control the strength of the drainage, where low values result in a well-drained column and high values result in a poorly or completely undrained column. A d^{lat} value of 10^4 m is used for *undrained* cases, which emulates conditions at a mostly flat surface. In reality this corresponds to no drainage, resulting in a one-dimensional case for the water balance, where only surface water is removed. For the *drained* cases, a d^{lat} value of 1 m is used, which emulates well-drained conditions at a slope.

165 The snow model used in this study was introduced by Zweigel et al. (2021) and is based on the CROCUS snow scheme (Vionnet et al. 2012). Snowfall is added on the surface with density and grain properties derived from atmospheric forcing data and then undergoes transient evolution of snow grains and density. The snow albedo undergoes a transient evolution in this snow scheme. The physical effect of wind drift on the snowpack is included in the module as well. Energy and mass transfer in the snowpack includes heat conduction, percolation of rainfall and percolation of meltwater (Westermann et al., 2022). The amount of snow can be adjusted by a so-called *snowfall factor*, sf , with which the snowfall from the model forcing is multiplied. With this, it is possible to phenomenologically represent redistribution of snow by wind (as in Martin et al., 2019) and to account for potential biases in the snowfall forcing. In this study, we conduct a sensitivity analysis towards the winter snow cover by selecting different values for sf .



Ground and snow parameters are kept constant in all model runs. For the ground we used an albedo of 0.15, emissivity
175 of 0.99, a roughness length of 10^{-3} m and a hydraulic conductivity of 10^{-5} m s⁻¹. For snow, we used an emissivity of 0.99, a
roughness length of 10^{-3} m, a hydraulic conductivity of 10^{-4} m s⁻¹ and a field capacity of 0.05 (see Westermann et al., 2022).

3.2 Validation, equilibrium and transient runs

Three types of CryoGrid simulations are distinguished, i.e. *validation runs*, *equilibrium runs* and *transient runs*. The *validation*
180 *runs* are set up to compare modelled ground temperatures with available field measurements at the two sites. At Juvvasshøe,
measurements consist of borehole data from 2000 to 2019, allowing a comparison at different depths. At the rock glacier in
Ivarsfjorden, comparison of model results with in situ measurements is accomplished with the available ground surface
temperature monitoring network (Lilleøren et al., 2022), using the loggers within the rock glacier outline and with continuous
measurements. The *equilibrium runs* aim to investigate the effect of three idealized stratigraphies under a range of different
amounts of snowfall on the ground thermal regime and ground ice table for a stable climate, using looped model forcing from
185 the years 2000–2010 at Juvvasshøe and 1960–1970 at the Ivarsfjorden rock glacier. Each stratigraphy is modelled for both the
undrained and *drained* cases, resulting in six scenarios. The goal of the *transient runs* is to analyze how the ground
temperatures and ground ice table may have developed from 1951 to 2019 under these different model setups.

3.3 Ground stratigraphy and snow

The porosity of the ground material and the thickness of sediment are important factors for the capacity of the ground to hold
190 water. Three idealized ground stratigraphies are set up in order to investigate the effect of water drainage on the ground thermal
regime and ground ice dynamics. These are referred to as the *blocks only*, *blocks with sediment* and *sediment only* stratigraphies
(Table 1) in the following. In all stratigraphies, bedrock is assumed below 5 m depth. Also, the bedrock properties of 3%
porosity and saturated conditions are kept constant throughout the study, which is in agreement with Hipp et al. (2012) and
Farbrot et al. (2011).

195 The *blocks only* stratigraphy consists of a coarse block layer with 50% porosity of 5 m thickness on top of bedrock.
The coarse blocks have a low field capacity of 1% (Table 1), which means that almost all water drains first downwards and
then laterally for the drained case. This idealized stratigraphy roughly corresponds to an active rock glacier where finer
sediments that result from weathering and erosion processes are transported towards the tongue of the rock glacier.
Furthermore, Dahl (1966) observed that blockfields on slopes more often do not contain a fine sediment fraction between the
200 blocks in northern Norway. In the second stratigraphy, *blocks with sediment*, the voids between coarse blocks are filled by a
finer-grained sediment fraction (sand) with again 50% porosity, resulting in an overall porosity of 25% and a higher field
capacity as water is held in the finer pores of the sediment fraction. Finally, the *sediment only* stratigraphy contains sand with
the same porosity as *blocks only*, but a higher field capacity again due to the water holding capacity of the fine-grained sediment
material.

205



Table 1: Three idealized subsurface stratigraphies. The values indicate the volumetric fractions of the soil constituents.

Depth (m)	Mineral	Organic	Porosity	Field capacity	Soil freezing
<i>Blocks only</i>					
0–5	0.5	0.0	0.5	0.01	Free water
<i>Blocks with sediment</i>					
0–5	0.75	0.0	0.25	0.15	Free water
<i>Sediment only</i>					
0–5	0.5	0.0	0.5	0.25	Sand

A changing snow cover is the main source of spatial variability in ground temperatures in Norwegian mountains (Gisnås et al., 2016). Following these studies, the sensitivity of the scenarios to different amounts of snowfall. All model runs use the same snow model, but the snowfall factor sf is adjusted to change the thickness of the winter snowpack.

Validation runs. For the validation runs with the borehole data in Juvvasshøe, different stratigraphies were manually tested until a good visual fit between modelled and measured ground temperatures at 2.0 m and 0.4 m depth was established. Based on observations of blocks and smaller cobbles with finer sediments down to the onset of bedrock at a depth of 5 m (Isaksen et al. 2003), the *blocks with sediment* stratigraphy is used as a starting point and the mineral content is increased in order to achieve a better fit. As this site is extremely exposed to wind and most snow is blown away (Isaksen et al. 2003; Westermann et al., 2013), the snowfall factor is set to values smaller than 1. The stratigraphies used for comparison to field measurements at the rock glacier in Ivarsfjorden are the *blocks with sediment* and *sediment only*, in addition to a two-layered blockfield stratigraphy used in a previous modeling study on ground temperatures in blockfields (see Table 1, Westermann et al., 2013). All loggers except for one are placed on the relict surface of the rock glacier (Lilleøren et al., 2022), where the surface does not consist of just coarse blocks, but also contains finer sediment in between. Here, the *blocks with sediment* and *sediment only* stratigraphy are considered most appropriate.

Equilibrium runs. The equilibrium runs simulate the equilibrium ground temperature for the three idealized stratigraphies in both the *drained* and *undrained* case. For each scenario, CryoGrid is run with snowfall factors of 0.0, 0.25, 0.5, 0.75, 1.0 and 1.5. This approach allows for an estimation of the threshold amount of snow above which permafrost will no longer exist in each of the six scenarios. Note that for all snowfall factors in this study, the snow pack fully melts in all years; only for sf values exceeding 2 at Juvvasshøe, the snowpack survives the summer in some years, eventually forming a perennial snow/ice patch.

Transient runs. The same three idealized stratigraphies are used to simulate the transient change in ground temperature and ground ice content over the period 1951 to 2019. This allows to investigate the susceptibility to ground warming/thawing



230 in a period when a significant increase air temperatures occurred at the two sites. For each of the sites, the best fitting snowfall
factor from the validation runs is chosen for the transient analysis.

3.4 Model forcing data and downscaling routine for climate data

235 The meteorological data used to force the CryoGrid model were generated by applying TopoSCALE, a topography-based
downscaling routine (Fiddes and Gruber, 2014), to ERA5 reanalysis data (Hersbach et al., 2020). ERA5 outputs are provided
as interpolated point values on a regular latitude-longitude grid at a resolution of 0.25° at an hourly frequency, both at the
surface level, corresponding to Earth's surface as represented in the reanalysis, and at 37 pressure levels in the atmosphere
from 1000 to 1 hPa. We considered data for the reanalysis period from 1951 to 2019. From the surface level we obtained: 2
meter air and dewpoint temperature, 10 meter meridional (northward) and zonal (eastward) wind velocity components, surface
240 pressure, constant surface geopotential, incoming longwave radiation, incoming shortwave radiation, and total precipitation.
From the pressure levels we acquired: air temperature, specific humidity, zonal and meridional wind velocity components, and
dynamic geopotential. For Juvvasshøe at 1894 m a.s.l. we used all levels in the range 900 hPa to 700 hPa, while for the lower
elevation Ivarsfjorden rock glacier at 60–160 m a.s.l. we used all levels between 900 hPa and 1000 hPa.

245 Terrain parameters derived from a digital elevation model (DEM) are needed to apply topography-based downscaling
to the ERA5 data. We obtained these parameters by processing the mosaic version of the ArcticDEM with a resolution of 32
m (Porter et al., 2018) at the respective sites. Based on the ERA5 data and the DEM-derived parameters we performed a
topography-based downscaling using the TopoSCALE routine. TopoSCALE is routinely used to downscale atmospheric
reanalysis data in complex terrain and has since been used in several cryospheric applications including estimating mountain
permafrost distribution (Fiddes et al., 2015), snow data assimilation (Aalstad et al., 2018), hyper-resolution snow reanalysis
250 (Fiddes et al., 2019), and downscaling regional climate model output (Fiddes et al., 2022).

By applying TopoSCALE all the necessary meteorological forcing fields required to run CryoGrid are retrieved: near
surface air temperature, specific humidity, wind speed, incoming longwave radiation, incoming shortwave radiation, as well
as snowfall and rainfall.

3.5 Model initialization

255 For the *validation runs* both at Juvvasshøe and Ivarsfjorden, the model is run for the entire period of available forcing data. At
Juvvasshøe the initial ground temperature profile is taken from the borehole data. At Ivarsfjorden the model is initialized to
near equilibrium conditions with the first 10 years of available forcing data. At Juvvasshøe, we compare the years 2010 to
2019 to measurements, while 2016 to 2019 is used for Ivarsfjorden. This leaves at least 60 years for the model spin-up which
is sufficient to analyze ground temperatures in uppermost meters of the ground column.

260 In order to reach steady state conditions in the *equilibrium runs*, a 10 year period of roughly stable climate is chosen
and iterated three times until a steady state temperature profile of the upper 5 meters is established. For Juvvasshøe, the period
2000–2010 is selected as the model can be initialized with real-time borehole data. For the Ivarsfjorden steady-state runs the



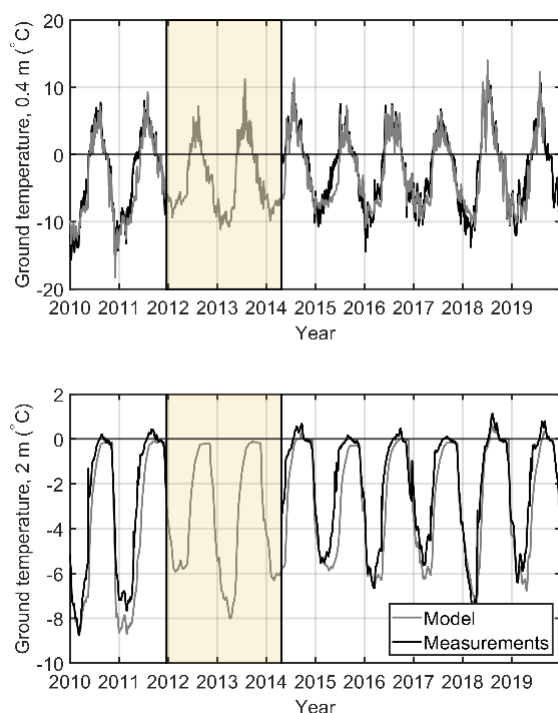
comparatively cold period 1960–1970 is selected as this relatively stable period is more likely to represent permafrost conditions than the other periods.

265 The goal of the *transient runs* is to investigate the warming and possible degradation of permafrost and ground ice melt from the second half of the 20th century until present for the different model scenarios, so that the rates of warming/thawing can be compared. For this purpose, an initialization procedure that allows the build-up of a stable ground ice table is required. This is achieved by iterating three times over the coldest 10 year period in the forcing data, from 1962 to 1971, until equilibrium conditions with a stable ice table are present. This is the coldest period in the available forcing data and thus the closest to Little Ice Age conditions, when the rock glacier Ivarsfjorden is hypothesized to have been active (Lilleøren et al., 2022). Steady-state simulations for this initialization period are then followed by the transient simulations for the entire forcing dataset from 1951 to 2019. Transient runs for Juvvasshøe are set up by the same procedure, using the coldest period 1962 to 1971 for spin-up.

4. Results

275 4.1 Comparison to in-situ measurements

Model results of the *validation runs* at Juvvasshøe are compared with measured ground temperatures at the PACE borehole (Etzelmüller et al., 2020). Figure 2 shows the comparison of measured ground temperatures with modelled temperatures at 2 m and 0.4 m depth for the best fitting model configuration. The snowfall factor for this model setup is 0.25, meaning the model reduces incoming snow by 75% in order to capture the effect of snow ablation due to wind drift. This resulted in mean annual maximum snow depths of 34 cm, in broad agreement with observations from the site (Iskasen et al., 2003) and earlier modeling studies at the site (Westermann et al., 2013). The subsurface stratigraphy for the best-fitting model configuration is highly similar to the *blocks with sediment* stratigraphy, but with a slightly lower porosity of 0.2 (i.e. a volumetric mineral content of 0.8) and an accordingly lower field capacity of 0.1. This would for example correspond to blocks and cobbles with a porosity of 0.4 (0.5 for *blocks with sediment*), filled with fine sediments with a porosity of 0.5 (and field capacity 0.25), which is plausible given the broad characteristics of the observed borehole stratigraphy (Isaksen et al., 2003). At 2 m depth, the simulations have a slight cold bias for the annual maxima close to 0 °C. The model simulates temperatures at 2 m depth better than at 0.4 m depth, as the effect of the strong variability of the ground surface temperature likely due to variations in the snow cover is dampened. Furthermore, the uppermost 1 m contain large stones and boulders, while the layer below is characterized by smaller stones and cobbles, so that a stratigraphic model with two layers in the uppermost 5 m might possibly yield an even better fit.



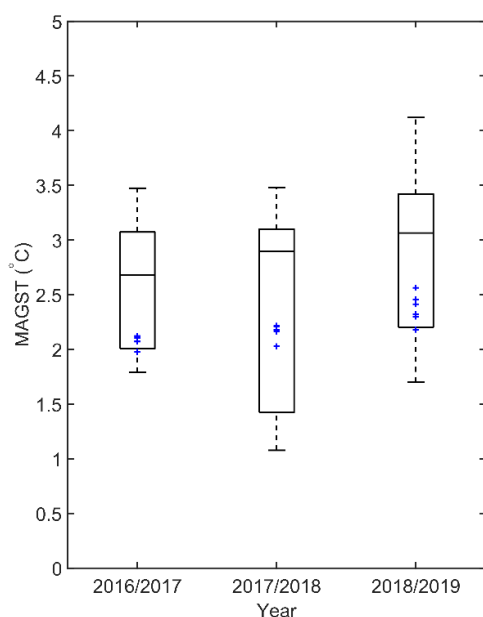
295 **Figure 2: Modelled and measured ground temperature at the PACE borehole in Juvvasshøe at 0.4 m (upper) and 2.0 m (lower) depth. The shaded area indicates a period when no borehole data are available.**

At the rock glacier in Ivarsfjorden, no borehole data are available. Therefore, a comparison between modelled and measured temperature is performed with data from a ground surface temperature logger network (Lilleøren et al., 2022). As this site is characterized by complex microtopography with likely strong variability of the snow cover (for which no observations are available), we focus on mean annual ground surface temperatures (MAGST) for individual years instead of a
300 time-resolved comparison as for Juvvasshøe. The three years of data at 11 locations on and near the rock glacier are presented together with six model *validation runs* (Fig. 3). These consist of two idealized stratigraphies (Sect. 3.3), in addition to the blockfield stratigraphy (see Table 1, Westermann et al., 2013) each in a *drained* and *undrained* configuration with a snowfall factor 1.0. There is likely a variable snow depth across the different parts of the rock glacier, which possibly explains part of the differences between modelled and measured temperatures.

305 Measured MAGST are in the range of 1.1 °C and 4.1 °C, while modelled MAGST are confined in a narrower range between 2.0 °C and 2.7 °C. For all years combined, the mean of the measurements is 2.7 °C, while the mean of all model realizations is 2.2 °C. We emphasize that the simulations all use a single snowfall factor and identical surface conditions, which likely explains the smaller range of simulated temperatures. In reality, the loggers are distributed in an area where small scale spatial variations in topography, snow accumulation, ground stratigraphy and vegetation play a role. While there are
310 some deviations between measurements and simulation results at both Juvvasshøe and Ivarsfjorden, we conclude that the



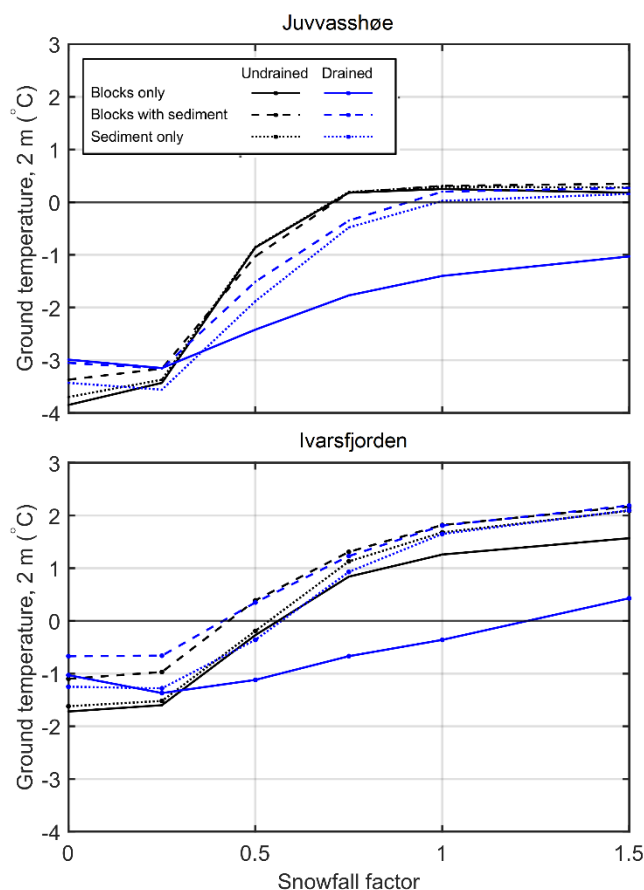
model setup (including the model forcing) can capture the general ground surface temperature regime at both sites which is a prerequisite for obtaining meaningful results from the *equilibrium* and *transient runs*.



315 **Figure 3: Modelled and measured MAGST in Ivarsfjorden during three years, from 13 July 2016 to 12 July 2019. The bars indicate the 25th and 75th percentile of measured MAGST and the whiskers represent the maximum and minimum temperatures. The blue indicators show modelled MAGST during the same period for a selected range of ground stratigraphies at $sf = 1$.**

4.2 Equilibrium ground temperatures and sensitivity to snow

320 Annual maximum snow depths at a snowfall factor of 1.0 are between 1.5 m and 2.4 m at Juvvasshøe and between 0.4 m and 1.0 m at Ivarsfjorden. Figure 4 shows the equilibrium ground temperature at 2 m depth for the three stratigraphies at different snowfall factors at both sites. For each of the three stratigraphies there is the *drained* and the *undrained* scenario. At both sites there is a clear pattern of lower temperatures in the *blocks only, drained* scenario (solid blue line) compared to all 5 other scenarios. For snowfall factors of 0.75 and larger, the difference in ground temperature between *blocks only, drained* and the other scenarios is in the range of 1.1 °C and 1.8 °C at Juvvasshøe and in the range of 1.1 °C and 2.2 °C at Ivarsfjorden.



325

Figure 4: Equilibrium ground temperature at 2 m depth for three idealized stratigraphies (Table 1) and different snowfall factors.

At Juvvasshøe, all three undrained scenarios feature positive ground temperatures at snowfall factors of 0.75 and above, which corresponds to permafrost-free conditions. Temperatures in the *blocks with sediment, drained* and *sediment only, drained* runs are positive for a snowfall factor of 1.0 and above. The ground temperature in the *blocks only, drained* runs remains below -1.0 °C for all snowfall scenarios. A similar pattern is seen in Ivarsfjorden, although a snowfall factor of 1.5 results in positive temperatures for the scenario *blocks only, drained* which is clear evidence of the overall warmer ground temperatures. Temperatures for the *blocks with sediment* stratigraphy are positive for snowfall factors exceeding 0.5, and exceeding 0.75 for the other scenarios (with the exception of the *blocks only, drained* scenario, see above). For snowfall factors above 0.25, ground temperature at 2 m depth increase with snow depth as a result of increased insulation. However, the increase from a snowfall factor of 0 to 0.25 leads to a slight cooling for the *drained* scenarios as opposed to a slight warming in the *undrained* scenarios. The reason for this cooling is likely the higher winter albedo of the completely snow-free ground (for snowfall factor zero), which outweighs the insulating of the shallow snow cover for snowfall factor 0.25.

330

335



340 Fig. 5 shows simulated temperatures for one year at the ground surface and 2 m depth for drained conditions for both
345 *blocks only* and the *blocks with sediment* scenarios for Juvvasshøe (snowfall factor 0.75). While ground surface temperatures
are largely similar during the snow-free summer season, they decrease much faster for the *blocks only* compared to the *blocks with sediment*
scenario, where the slow refreezing of the active layer leads to a prolonged warming of the ground surface from
below. In the *blocks only* scenario, on the other hand, the active layer contains only little water, so that refreezing occurs within
only a short time period. The rapid cooling in the *blocks only* scenario is also visible within the permafrost table at 2 m depth,
resulting in lower winter temperatures compared to the *blocks with sediment* curve and thus explaining the simulated
differences in MAGT.

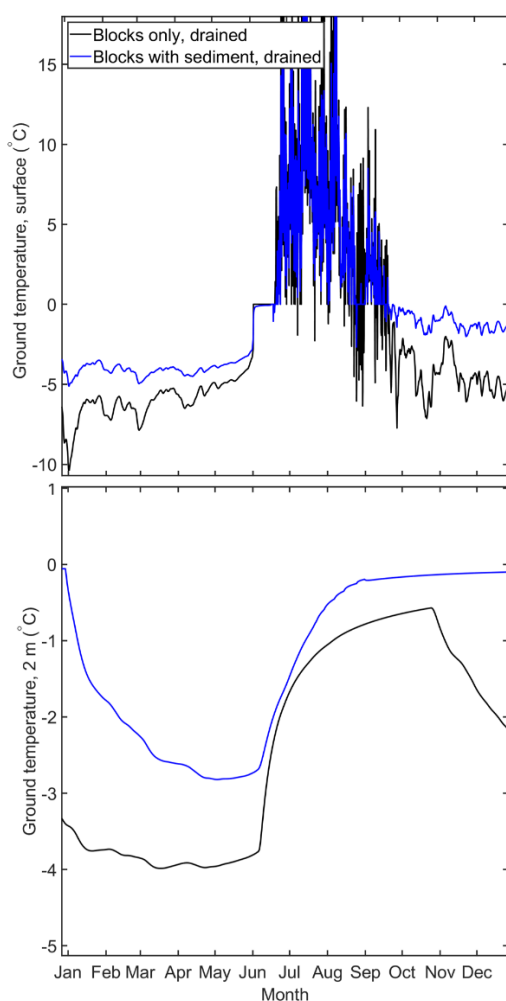
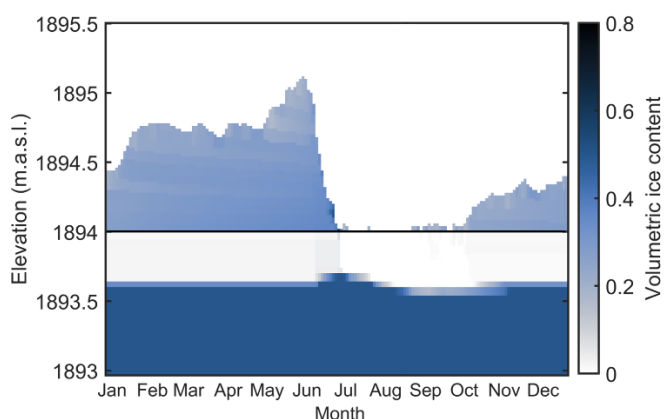


Figure 5: Modelled ground temperature at 0.05 m (top) and 2 m (bottom) depth for the *blocks only, drained* and *blocks with sediment, drained* scenarios during a year of an equilibrium run at Juvvasshøe. $S_f = 0.75$.



350 Figure 6 shows the corresponding snow cover and volumetric ground ice content in the upper meter of the ground for the *blocks only, drained* scenario. A largely stable ground ice table forms already at a depth of about 0.5 m, while the active layer is almost free of ground ice in winter, corresponding to the low water content enabling rapid refreezing and thus strong cooling during winter. During and after snow melt, meltwater infiltrates in the blocky layer and refreezes at the then very cold ice table, resulting in the formation of new ground ice which slowly melts during the course of summer. The slight increase of
355 the ground ice table in early winter is due to refreezing of residual water above the ice table from rain and snow melt events in October which has not fully drained before refreezing.



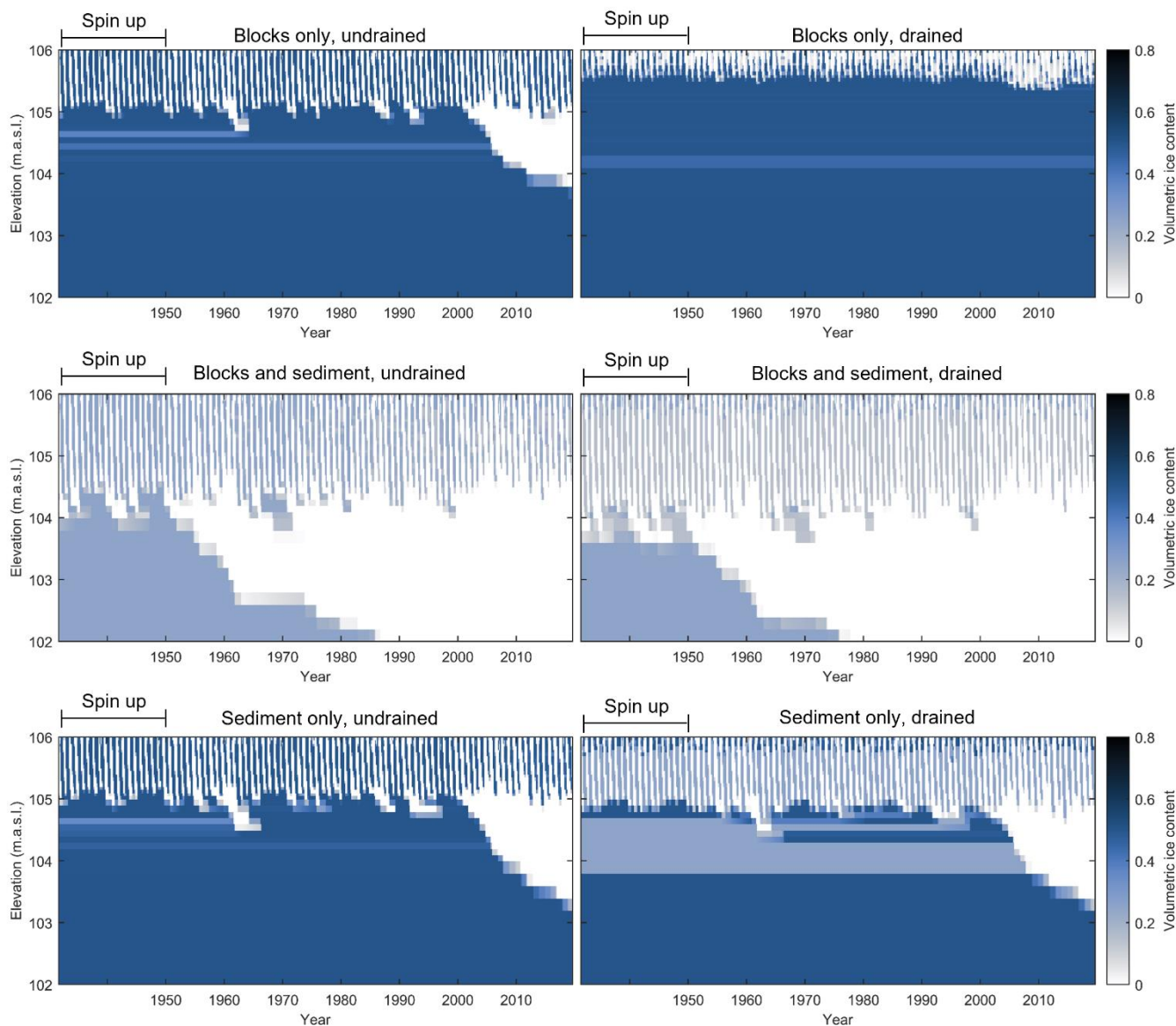
360 **Figure 6: Modelled volumetric ground ice content in the upper 1 m of the ground (<1894m) and the snow cover (>1894m) for the *blocks only, drained* scenario, during one year of an equilibrium run at Juvvasshøe. Note the rise of the ground ice table in June after infiltrated snow melt water refreezes. $S_f = 0.75$.**

4.3 Transient response of ground temperatures and ice content

The ERA5 reanalysis dataset allows us to model the evolution of the ground thermal regime and ground ice content from 1951 to 2019. Figure 7 shows the ground ice content for the different scenarios in Ivarsfjorden. In all simulations, a stable ice table and permafrost conditions form during the spin up period, with volumetric ice contents of 0.5 (*blocks only, sediment only*) and
365 of 0.25 (*blocks with sediment*) according to the applied stratigraphy (table1). In the period 1951 to 2019, ground ice contents evolves as a response to the applied climate forcing, showing different responses of the ground ice table. In the *blocks only, drained* scenario, the ice table does not lower by a significant amount, while the ice table lowers significantly in all other simulations. The perennial ice table in the upper 5 m of the *blocks with sediment* stratigraphy disappeared by 1985 and 1975 in the *undrained* and *drained* scenarios respectively. Finally, the *sediment only* simulations show an intermediate effect where
370 the ice table has dropped to approximately half of its initial height by 2019. We conclude that the ground stratigraphy and drainage conditions strongly control the response of the ground towards warming, with full degradation near-surface permafrost in both *blocks with sediment* runs, partial degradation in the *blocks only, undrained* run and in both *sediment only*



runs and finally continued stable permafrost conditions in the *blocks only, drained* simulation. At the Juvvasshøe site, the ice table persists in all simulations, but a slight lowering occurs in the *blocks with sediment* scenarios.



375

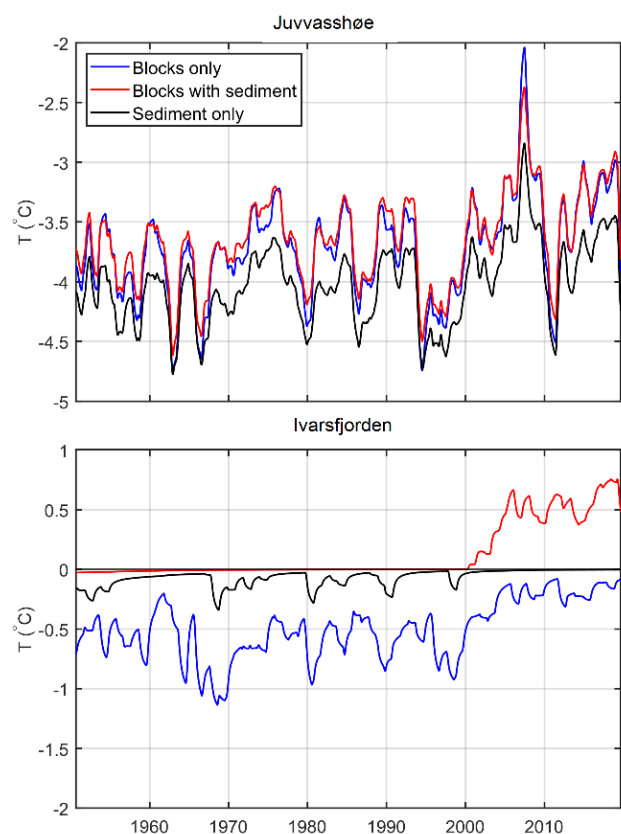
Figure 7: Modelled volumetric ground ice content at Ivarsfjorden for the idealized stratigraphies in *undrained* and *drained* conditions. The $sf = 1.0$ in all simulations.

The changes in ground temperature are also strongly dependent on the stratigraphy. Figure 8 shows the change in temperatures at 5 m depth for the *drained* scenarios, which at the Ivarsfjorden rock glacier (snowfall factor 1.0) correspond to a full (*blocks with sediment*) and partial (*sediment only*) lowering, as well as a relatively stable (*blocks only*) ice table. The *blocks only* simulation underwent an increase from -0.6 °C to -0.2 °C between the 1951–1960 and 2010–2019 means, not being

380



385 strongly influenced by latent heat effects due to the relative stable ice table. The *sediment only* case experienced minimal warming in this period at 5 m depth, strongly influenced by the ongoing ground ice melt which confines ground temperatures to close to 0 °C. Finally, the complete degradation of the ice table in *blocks with sediment* run coincided with a warming to positive temperatures, from 0.0 °C to 0.6 °C. Ground temperatures at 5 m depth were lower for snowfall factor 0.5 and resulted in less ice melt, so that the warming between the 1951–1960 and 2010–2019 means were from -0.8 °C to -0.3 °C in the *blocks only* stratigraphy, from -0.5 °C to 0.0 °C in the *sediment only* stratigraphy and from -0.1 °C to 0.1 °C in the *blocks with sediment* stratigraphy.



390 **Figure 8:** Ground temperature at 5 m depth for the idealized stratigraphies under *drained* conditions. $sf = 1.0$ for Ivarsfjorden and $sf = 0.25$ for Juvvasshøe.

395 At Juvvasshøe, permafrost degradation and thus strong ground ice melt does not occur for any of the scenarios for snowfall factor 0.25 (Fig. 8). Nevertheless, the warming rates differed to some degree between the scenarios. In the *blocks only* simulation, 5m ground temperatures increased from -3.7 °C to -3.5 °C between the 1951–1960 and 2010–2019 means, from -3.8 °C to -3.4 °C for the *blocks with sediment* run ranged and from -4.1 °C to -3.7 °C in the *sediment only* run. For snowfall factor 0.5, the change in temperature at 5 m depth in *drained* scenarios were overall higher, i.e. from -3.1 °C to -2.6



°C for the *blocks only* stratigraphy, from -2.5 °C to -1.9 °C for the *blocks with sediment* stratigraphy and from -2.9 °C to -2.4 °C for the *sediment only* stratigraphy. In conclusion, the warming rates appear more sensitive to changes in the amount of snowfall than to differences in the stratigraphy and drainage conditions, unless permafrost degradation and thus strong ground ice melt occur which is accompanied by low rates of warming.

5. Discussion

5.1 Limitations of the model setup

In this study, CryoGrid has been applied at two permafrost sites in mountain environments. At both sites, we set up validation runs to benchmark the performance of model system against measurements of ground (Juvvasshøe) and ground surface (Ivarsfjorden) temperatures. At Juvvasshøe, the model can largely reproduce the annual cycle of measured ground temperatures at the PACE borehole, when the snowfall is reduced to account for the generally shallow snow cover at the site. At Ivarsfjorden, the simulations for the *blocks only*, *drained* scenario are in broad agreement with observations at the rock glacier which indicate that permafrost is or has been present in the recent past (Lilleøren et al., 2022). This is remarkable as the site is located far outside the mapped permafrost range (e.g. Gislås et al., 2017), which is corroborated by the other scenarios (representing “normal” ground) in which near-surface permafrost no longer exists. Modelled MAGSTs fall within the 25th and 75th percentile of measured MAGSTs between July 2016 and July 2019. However, modelled MAGSTs are colder than the mean and median measurements, indicating a small potential bias of the model of approximately -0.5 °C. Within the model setup, in particular the exact ground stratigraphy and other poorly constrained parameters, such as the albedo, give rise to uncertainties when comparing to measurements. Only at Juvvasshøe, the stratigraphy has been described from the borehole (Isaksen et al., 2003), while no thorough evaluation of the subsurface stratigraphy is available for Ivarsfjorden. Lilleøren et al. (2022) described the site as a complex creeping system with inhomogeneous subsurface properties. Most of the rock glacier surface is described as ‘relict’ (Lilleøren et al., 2022) with sand and gravel in between blocks. For these ‘relict’ areas, the simulations for the *blocks with sediment* and *sediment only* stratigraphy, in which near-surface permafrost fully or partially degrades, could indeed represent the thermal state adequately. Two areas are described as ‘fresh’ which could indicate lateral movements due to the presence of ground ice. These contain larger blocks and could thus be better described by the *blocks only* stratigraphy for which permafrost and ground ice still persist at the end of the simulations. However, also in these ‘fresh’ areas, the amount of finer sediment is unclear, in particular in deeper layers. In our simulations, we have only considered a single, homogeneous layer in the uppermost 5 m in order to compare the thermal regime and ground ice dynamics for idealized stratigraphies. In reality, ground stratigraphies in blocky terrain can feature aspects of all scenarios, for example a blocky layer with air-filled voids on top, followed by blocks filled with sediments and a sediment only layer in the bottom. For the cooling effect described in this study, it is critical that the blocky top layer is deep enough so that a ground ice table from which water can drain can form within. Therefore, it is likely that also shallower blocky layers with air-filled voids can lead to lower ground temperatures, depending on the climatic conditions which determine the depth of the ground ice table.



We emphasize that a consistent model setup was selected for all scenarios, so that uncertainties caused by other parts
430 of the model system influence them all in a similar, consistent way. In particular, none of the convective processes summarized
by Harris and Pedersen (1998) that cause a negative thermal anomaly in blocky terrain are considered in the model setup. The
same applies to the effect of rocks protruding into and through the snow cover as was described by Juliussen and Humlum
(2008) which could potentially be included in CryoGrid by laterally coupled simulations (e.g. Zweigel et al. 2021) with snow
redistribution between tiles representing blocks of different heights. Considering air convection in future simulations (as e.g.
435 in Wicky and Hauck, 2017) should become a priority for model development as this is likely to interact with the ground ice
mass balance for the blocky drained scenario and could thus exacerbate the thermal anomaly.

Further uncertainties are related to the model forcing data. The ERA5 reanalysis data is a global product with coarse
horizontal resolution, so that the TopoSCALE downscaling routine (Fiddes and Gruber 2014) is applied to obtain more
representative meteorological forcing. Nonetheless, as mentioned in Fiddes and Gruber (2014) as well as Fiddes et al. (2019)
440 and Fiddes et al. (2022), there are also some limitations to this scheme, in particular the primitive downscaling scheme for
precipitation, which only interpolates between ERA5 grid points and thus misses the effects of local orography. The same is
true for the effects of local cloud build-up around slopes and mountains, which affects the radiation budget. While these
uncertainties could affect the comparison of model results to field measurements (Sect. 4.1), the model forcing data can
certainly capture the regional-scale climate characteristics of the two study sites, e.g. the significant differences in MAAT
445 between the two sites. The thermal anomaly of the *blocks only, drained* scenario consistently occurs for both sites and thus
over a significant range of climate conditions, so that the effect is likely robust despite the uncertainties in the model forcing
data. The same is true for the uncertainty caused by the Crocus-based snow (Vionnet et al. 2012; Zweigel et al., 2021). In this
study, we have performed a sensitivity study with respect to the amount of snow (by modifying the snowfall factor, Sect. 4.2),
but simply scaling snowfall cannot represent the true time evolution of the snow cover due to wind redistribution (e.g. Liston
450 & Sturm, 1998; Martin et al., 2019). Nevertheless, it seems unlikely that the exact time dynamics of snow ablation and/or
deposition events strongly affects the dependence of the thermal anomaly in the *blocks only, drained* scenario on overall
winter snow depths.

5.2 The effect of the ground ice dynamics on ground temperatures

Despite the uncertainties of the model setup, our results show a clear negative thermal anomaly for the *blocks only, drained*
455 scenario. If the winter snow depth is sufficiently high, a surface cover of coarse blocks with air-filled voids (i.e. high porosity
and low water holding capacity) results in 2 m ground temperatures 1 to 2 °C lower than for the other stratigraphies. In the
Ivarsfjorden simulations, the *blocks only, drained* scenario is the only one where near-surface permafrost conditions persist
even today, while near-surface permafrost degrades for the *blocks with sediment* and *sediment only* scenarios. This is
accompanied by a strong thermal offset, with a MAGST of more than 2 °C for the *blocks only, drained* scenario, while MAGT
460 at 2 m were below 0 °C. Interestingly, the temperature anomaly appears largely constant over time in the transient simulations,
except for periods when permafrost disappears in one of the scenarios and confines ground temperatures to 0 °C, which delays



further ground warming. For lower snow depths, the temperature anomaly becomes smaller and eventually vanishes for the (generally irrelevant) case of permanently snow-free conditions.

The negative temperature anomaly largely accumulates during fall and winter (Fig. 5). As the active layer contains
465 very little water in the *blocks only, drained* scenario, it rapidly refreezes during fall which enables a fast cooling of the deeper soil layers and thus leads to overall lower winter temperatures. In spring, this “cold content” (i.e. sensible heat) of the ground is partly transformed into the build-up of new ground ice (i.e. latent heat, Fig. 6) which only melts slowly during summer due to the insulation of the overlying blocky layer. This timing of the ground ice formation is strongly different from all other scenarios, for which ground ice mostly forms in fall/early winter due to refreezing of the water contained in the active layer.
470 This refreezing of the active layer can take several months and is further delayed if a significant snow cover forms during this period, which leads to overall higher winter temperatures in the permafrost. It is exactly for these “high-snow situations” (corresponding to higher snowfall factors in our sensitivity analyses) that the temperature anomaly of the *blocks only, drained* scenario is largest. Our results suggest that permafrost can occur for blocky ground on slopes around Juvvasshøe, even if the winter snow cover exceeds 2 m thickness.

We note that the thermal anomaly caused by the ground ice dynamics in blocky ground is not related to convective
475 processes (Harris and Pedersen, 1998) or the effect of blocks protruding through the snow cover (Juliussen and Humlum, 2008; Gruber Hoelzle, 2008). A somewhat similar effect has been described for peat plateaus in northern Norway where simulations yielded 2 °C lower temperatures for well-drained peat compared to water-saturated peat (Martin et al., 2019). The simulated temperature anomaly is similar to the 1.3–2.0 °C lower temperatures that Juliussen and Humlum (2008) found in blockfields
480 compared to till and bedrock in Central-eastern Norway. While a complete process model for blocky ground and rock glaciers will certainly have to take air convection and the interplay between surface blocks and the snow cover into account, it is encouraging, the relatively simple model approach presented in this work offers prospects to improve our estimates of permafrost occurrence in mountain environments.

In a first-order approach, thermal anomalies can be translated into elevation differences by assuming a temperature
485 lapse rate, so that the impacts on the lower altitudinal limit of permafrost can be estimated. For a lapse rate of 0.5 °C per 100 m (e.g. Farbrot et al., 2011), the lower limit of permafrost in drained, blocky deposits in Norway would be 300 to 400 m lower compared to “normal” permafrost represented by the other scenarios. For the Ivarsfjorden site, these numbers compare favorably to the Scandinavian permafrost map (Gisnås et al., 2017) which shows a lower discontinuous permafrost limit in Finnmark at around 400 m a.s.l., approx. 300 m above the rock glacier.

490 5.3 Implications for future work

In this study, we show that modelling the full subsurface water and ice balance in well-drained blocky deposits with air-filled voids leads to significantly lower ground temperatures in permafrost environments. In modelling studies on the distribution of permafrost, blocky ground usually is not accounted for, or the water balance is not simulated at this level of detail. For the Northern hemisphere permafrost map (Obu et al., 2019), a coarse landcover classification was used in mountain areas which



495 did not represent blocky terrain. To produce the map, a semi-empirical equilibrium TTOP model was used in which the thermal
anomaly of blocky deposits likely could account for by adjusting the r_k parameter which accounts for the thermal offset of the
ground. A more sophisticated modelling approach as presented in this work could be used to train the more simple TTOP
model across a range of climate conditions. Permafrost mapping with transient models (e.g. Jafarov et al., 2012) often uses
500 fixed ground stratigraphies, in which the sum of water and ice contents does not change for a given layer. An example is the
transient permafrost map for southern Norway (Westermann et al., 2013) which featured a dedicated stratigraphic class for
blocky deposits, with a dry upper layer followed by an ice-saturated layer below, very similar to the stratigraphy used for the
blocks only, drained scenario in this study. However, both layers have a fixed thickness and the sum of water and ice contents
is constant, so that the temporal evolution of ground ice dynamics cannot be captured. If the seasonal thaw extends in the ice-
rich layer, a pool of meltwater forms which cannot drain and hence strongly delays refreezing in fall, potentially resulting in
505 the degradation of permafrost. In our simulations with full water/ice dynamics, the ice table instead varies over time, both
seasonally and over longer periods in response to the climatic forcing. Such changes in the ground ice table have for example
been observed at the Schilthorn site in the European Alps where the ground ice table was significantly lowered during a hot
summer and did not regrow in the following years although permafrost conditions persisted (Hilbich et al., 2008). As the
observation site is located on a slope, it is clear that such observed ground ice dynamics can only be reproduced if lateral
510 drainage of meltwater is taken into account. To improve transient modelling of mountain permafrost distribution, CryoGrid in
the configuration used in this study could be adapted for individual grid cells, especially by adjusting the strength of the lateral
drainage (i.e. the distance to seepage face) depending on the local slope. In flat areas and depressions, water would then pool
up as for the *undrained* cases, while both melt- and rainwater would drain in sloping terrain as in the *undrained* cases, with
corresponding changes to the ground thermal regime and permafrost distribution. Furthermore, our study suggests that the
515 presence of fine sediments in the voids between blocks can strongly alter the ground temperature compared to blocky terrain
with air-filled voids. For spatially distributed mapping, these two cases would have to be distinguished as separate stratigraphic
classes and maps of their spatial extent must be available. Especially the latter is expected to be significant challenge, as the
surfaces likely appear similar for remote sensors, so that detailed field mapping may be required.

The model approach in this study also offers significant potential to study ground ice derived runoff from blocky
520 deposits and rock glaciers. While the Norwegian study sites are both located in wet climate settings with ample water supply,
rock glaciers in more arid regions can be important sources of water (e.g. Croce and Milana 2002). The global ratio of rock
glacier to glacier water volume equivalent (WVEQ) is currently increasing as both systems react differently to a changing
climate (Jones et al., 2019). Therefore, simulations of ground ice volumes and seasonal runoff characteristics in both the
present and future climates can be a valuable tool for the assessment of water resources. Furthermore, rock glaciers are sensitive
525 to climate change (Haerberli et al., 2010) and recent studies have linked rock glacier acceleration to increasing air temperatures
(e.g. Käab et al., 2007; Hartl et al., 2016; Eriksen et al., 2018). Our model approach is likely able to simulate the seasonal
ground ice mass balance at different points and elevations of a rock glacier which could be ingested in a flow model for rock
glaciers (e.g. Monnier and Kinnard, 2016). Finally, permafrost degradation and ground ice loss can also play an important role



for slope stability in mountain permafrost environments (e.g. Gruber and Haeberli, 2007; Saemundsson et al. 2018; Nelson et al., 2001). Simulations of ground ice table changes, as well as the occurrence of strong melt events with corresponding production of meltwater, could eventually improve assessments of the stability and hazard potential of permafrost-underlain slopes (e.g. Mamot et al., 2021).

6. Conclusions

In this study, we used the CryoGrid permafrost model to simulate the effect of blocky terrain on the ground thermal regime and ground ice dynamics at two Norwegian mountain permafrost sites (Juvvasshøe and Ivarsfjorden rock glacier). We used idealized stratigraphies and drainage conditions (referred to as ‘scenarios’) to investigate thermal anomalies for different amounts of snowfall. From this study, the following conclusions can be drawn:

- Markedly lower ground temperatures are found in well drained, coarse blocky deposits with air-filled voids (denoted *blocks only, drained* scenario) compared to other scenarios which are either undrained or feature fine sediments. The thermal anomaly is up to 1.8–2.2 °C, with largest values in simulations with thick winter snow cover. We emphasize that the model does not account for well-known factors, such as air convection and the effect of blocks protruding through the winter snow cover. The negative thermal anomaly is mainly linked to differences in the freeze-thaw dynamics caused by the removal of meltwater and the build-up of new ground ice in spring.
- For the *blocks only, drained* scenario, thermally stable permafrost can exist at the Ivarsfjorden site (located near sea level), even for a mean annual ground surface temperature (MAGST) of 2.0–2.5 °C. At Juvvasshøe in the southern Norwegian mountains, permafrost is simulated even for a very thick winter snow cover in the *blocks only, drained* scenario, while all other scenarios in this case feature permafrost-free conditions.
- Transient simulations since 1951 at the Ivarsfjorden rock glacier show a completely or partially degraded ground ice table for all scenarios, except the *blocks only, drained* scenario. This result is explained by the overall lower ground temperatures in this scenario, while the simulated warming rates are generally similar for all scenarios, except for periods when strong ground ice melt occurs.

This study suggests that including subsurface water and ice dynamics can drive simulations of mountain permafrost dynamics towards reality, which can for example improve estimates of the lower altitudinal limit of permafrost in blocky terrain. In addition to permafrost distribution mapping, the presented model approach could be used to simulate the seasonal and multi-annual evolution of the ground ice table, in addition to ground-ice derived runoff. It therefore represents a further step to a better understanding and model representation of the permafrost processes in mountain environments.



560 *Code and data availability.* The CryoGrid source code and model setup files are available
<https://doi.org/10.5281/zenodo.6563651> (Renette, 2022). Field measurements at Juvvasshøe are from Etzelmüller et al. (2020).
Field measurements at Ivarsfjorden are from Lilleøren et al. (2022).

Author contribution. CR performed the model simulations, retrieved forcing data, wrote the draft manuscript and created all
565 figures. SW helped design the study, developed the model and provided ideas throughout the entire study. KA developed code
for retrieving and downscaling forcing data, assisted with this process and wrote text regarding the forcing data. KL and KI
provided field measurements, site descriptions and photos. RBZ and JA developed parts of the model. All authors contributed
with text and suggestions.

570 *Competing interests.* The authors declare that they have no conflict of interest.

Acknowledgements. This work was supported by ESA Permafrost_CCI (<https://climate.esa.int/en/projects/permafrost/>),
Permafrost4Life (Research Council of Norway, grant no. 301639), and Nunataryuk (EU grant agreement no. 773421), as well
as the Department of Geosciences, University of Oslo.

575



References

- Aalstad, K., Westermann, S., Schuler, T. V., Boike, J., and Bertino, L.: Ensemble-based assimilation of fractional snow-covered area satellite retrievals to estimate the snow distribution at Arctic sites, *The Cryosphere*, 12, 247–270, <https://doi.org/10.5194/tc-12-247-2018>, 2018.
- 580 Arenson, L. U., Phillips, M., and Springman, S. M.: Geotechnical considerations and technical solutions for infrastructure in mountain permafrost, in: *New permafrost and glacier research*, pp. 3–50, Nova Science Publishers, 2009.
- Azócar, G. and Brenning, A.: Hydrological and geomorphological significance of rock glaciers in the dry Andes, Chile (27–33 S), *Permafrost and Periglacial Processes*, 21, 42–53, <https://doi.org/10.1002/ppp.669>, 2010.
- Croce, F. A. and Milana, J. P.: Internal structure and behaviour of a rock glacier in the arid Andes of Argentina, *Permafrost and Periglacial Processes*, 13, 289–299, <https://doi.org/10.1002/ppp.431>, 2002.
- 585 Dahl, R.: Block fields, weathering pits and tor-like forms in the Narvik Mountains, Nordland, Norway, *Geografiska Annaler: Series A, Physical Geography*, 48, 55–85, <https://doi.org/10.1080/04353676.1966.11879730>, 1966.
- Eriksen, H., Rouyet, L., Lauknes, T., Berthling, I., Isaksen, K., Hindberg, H., Larsen, Y., and Corner, G.: Recent acceleration of a rock glacier complex, Adjet, Norway, documented by 62 years of remote sensing observations, *Geophysical Research Letters*, 45, 8314–8323, <https://doi.org/10.1029/2018GL077605>, 2018.
- 590 Etzelmüller, B., Berthling, I., and Sollid, J. L.: Aspects and concepts on the geomorphological significance of Holocene permafrost in southern Norway, *Geomorphology*, 52, 87–104, [https://doi.org/10.1016/S0169-555X\(02\)00250-7](https://doi.org/10.1016/S0169-555X(02)00250-7), 2003.
- Etzelmüller, B., Schuler, T. V., Isaksen, K., Christiansen, H. H., Farbro, H., and Benestad, R.: Modeling the temperature evolution of Svalbard permafrost during the 20th and 21st century, *The Cryosphere*, 5, 67–79, [https://doi.org/10.5194/tc-5-67-](https://doi.org/10.5194/tc-5-67-2011)
2011, 2011.
- 595 Etzelmüller, B., Guglielmin, M., Hauck, C., Hilbich, C., Hoelzle, M., Isaksen, K., Noetzi, J., Oliva, M., and Ramos, M.: Twenty years of European mountain permafrost dynamics—the PACE legacy, *Environmental Research Letters*, 15, 104070, <https://doi.org/10.1088/1748-9326/abae9d>, 2020.
- Farbro, H., Hipp, T. F., Etzelmüller, B., Isaksen, K., Ødegård, R. S., Schuler, T. V., and Humlum, O.: Air and ground
600 temperature variations observed along elevation and continentality gradients in Southern Norway, *Permafrost and Periglacial Processes*, 22, 343–360, <https://doi.org/10.1002/ppp.733>, 2011.
- Fiddes, J. and Gruber, S.: TopoSCALE v. 1.0: downscaling gridded climate data in complex terrain, *Geoscientific Model Development*, 7, 387–405, <https://doi.org/10.5194/gmd-7-387-2014>, 2014.
- Fiddes, J., Endrizzi, S., and Gruber, S.: Large-area land surface simulations in heterogeneous terrain driven by global data sets:
605 application to mountain permafrost, *The Cryosphere*, 9, 411–426, <https://doi.org/10.5194/tc-9-411-2015>, 2015.
- Fiddes, J., Aalstad, K., and Westermann, S.: Hyper-resolution ensemble-based snow reanalysis in mountain regions using clustering, *Hydrology and Earth System Sciences*, 23, 4717–4736, <https://doi.org/10.5194/hess-23-4717-2019>, 2019.



- Fiddes, J., Aalstad, K., and Lehning, M.: TopoCLIM: rapid topography-based downscaling of regional climate model output in complex terrain v1. 1, *Geoscientific Model Development*, 15, 1753–1768, <https://doi.org/10.5194/gmd-15-1753-2022>,
610 2022.
- Gisnås, K., Etzelmüller, B., Lussana, C., Hjort, J., Sannel, A. B. K., Isaksen, K., Westermann, S., Kuhry, P., Christiansen, H. H., Frampton, A., et al.: Permafrost map for Norway, Sweden and Finland, *Permafrost and periglacial processes*, 28, 359–378, <https://doi.org/10.1002/ppp.1922>, 2017.
- Gisnås, K., Westermann, S., Schuler, T. V., Melvold, K., and Etzelmüller, B.: Small-scale variation of snow in a regional
615 permafrost model, *The Cryosphere*, 10, 1201–1215, <https://doi.org/10.5194/tc-10-1201-2016>, 2016.
- Gruber, S. and Haeberli, W.: Permafrost in steep bedrock slopes and its temperature-related destabilization following climate change, *Journal of Geophysical Research: Earth Surface*, 112, <https://doi.org/10.1029/2006JF000547>, 2007.
- Gruber, S. and Hoelze, M.: The cooling effect of coarse blocks revisited: a modeling study of a purely conductive mechanism, *Zurich Open Repository and Archive*, 2008.
- 620 Haeberli, W., Hallet, B., Arenson, L., Elconin, R., Humlum, O., Kääh, A., Kaufmann, V., Ladanyi, B., Matsuoka, N., Springman, S., et al.: Permafrost creep and rock glacier dynamics, *Permafrost and periglacial processes*, 17, 189–214, <https://doi.org/10.1002/ppp.561>, 2006.
- Hanson, S. and Hoelzle, M.: The thermal regime of the active layer at the Murtèl rock glacier based on data from 2002, *Permafrost and Periglacial Processes*, 15, 273–282, <https://doi.org/10.1002/ppp.499>, 2004.
- 625 Harris, C., Haeberli, W., Vonder Mühll, D., and King, L.: Permafrost monitoring in the high mountains of Europe: the PACE project in its global context, *Permafrost and periglacial processes*, 12, 3–11, <https://doi.org/10.1002/ppp.377>, 2001.
- Harris, C., Arenson, L. U., Christiansen, H. H., Etzelmüller, B., Frauenfelder, R., Gruber, S., Haeberli, W., Hauck, C., Hoelzle, M., Humlum, O., et al.: Permafrost and climate in Europe: Monitoring and modelling thermal, geomorphological and geotechnical responses, *EarthScience Reviews*, 92, 117–171, <https://doi.org/10.1016/j.earscirev.2008.12.002>, 2009.
- 630 Harris, S. A. and Pedersen, D. E.: Thermal regimes beneath coarse blocky materials, *Permafrost and periglacial processes*, 9, 107–120, [https://doi.org/10.1002/\(SICI\)1099-1530\(199804/06\)9:2<107::AID-PPP277>3.0.CO;2-G](https://doi.org/10.1002/(SICI)1099-1530(199804/06)9:2<107::AID-PPP277>3.0.CO;2-G), 1998.
- Hartl, L., Fischer, A., Stocker-waldhuber, M., and Abermann, J.: Recent speed-up of an alpine rock glacier: an updated chronology of the kinematics of outer hochebenkar rock glacier based on geodetic measurements, *Geografiska Annaler: Series A, Physical Geography*, 98, 129–141, <https://doi.org/10.1111/geoa.12127>, 2016.
- 635 Hersbach, H., Bell, B., Berrisford, P., Hirahara, S., Horányi, A., Muñoz-Sabater, J., Nicolas, J., Peubey, C., Radu, R., Schepers, D., et al.: The ERA5 global reanalysis, *Quarterly Journal of the Royal Meteorological Society*, 146, 1999–2049, <https://doi.org/10.1002/qj.3803>, 2020.
- Hilbich, C., Hauck, C., Hoelzle, M., Scherler, M., Schudel, L., Völksch, I., Vonder Mühll, D., and Mäusbacher, R.: Monitoring mountain permafrost evolution using electrical resistivity tomography: A 7-year study of seasonal, annual, and long-term
640 variations at Schilthorn, Swiss Alps, *Journal of Geophysical Research: Earth Surface*, 113, <https://doi.org/10.1029/2007JF000799>, 2008.



- Hipp, T., Etzelmüller, B., Farbrot, H., Schuler, T., and Westermann, S.: Modelling borehole temperatures in Southern Norway—insights into permafrost dynamics during the 20th and 21st century, *The Cryosphere*, 6, 553–571, <https://doi.org/10.5194/tc-6-553-2012>, 2012.
- 645 Humlum, O.: Active layer thermal regime at three rock glaciers in Greenland, *Permafrost and Periglacial Processes*, 8, 383–408, [https://doi.org/10.1002/\(SICI\)1099-1530\(199710/12\)8:4<383::AID-PPP265>3.0.CO;2-V](https://doi.org/10.1002/(SICI)1099-1530(199710/12)8:4<383::AID-PPP265>3.0.CO;2-V), 1997.
- Isaksen, K., Holmlund, P., Sollid, J. L., and Harris, C.: Three deep alpine-permafrost boreholes in Svalbard and Scandinavia, *Permafrost and Periglacial Processes*, 12, 13–25, <https://doi.org/10.1002/ppp.380>, 2001.
- Isaksen, K., Heggem, E., Bakkehøi, S., Ødegård, R., Eiken, T., Etzelmüller, B., and Sollid, J.: Mountain permafrost and energy
650 balance on Juvvasshøe, southern Norway, in: 8th International Conference on Permafrost, Zurich, Switzerland, ISI: 000185049300083, pp. 467–472, 2003.
- Isaksen, K., Sollid, J. L., Holmlund, P., and Harris, C.: Recent warming of mountain permafrost in Svalbard and Scandinavia, *Journal of Geophysical Research: Earth Surface*, 112, <https://doi.org/10.1029/2006JF000522>, 2007.
- Jafarov, E. E., Marchenko, S. S., and Romanovsky, V.: Numerical modeling of permafrost dynamics in Alaska using a high
655 spatial resolution dataset, *The Cryosphere*, 6, 613–624, <https://doi.org/10.5194/tc-6-613-2012>, 2012.
- Jones, D. B., Harrison, S., Anderson, K., and Whalley, W. B.: Rock glaciers and mountain hydrology: A review, *Earth-Science Reviews*, 193, 66–90, <https://doi.org/10.1016/j.earscirev.2019.04.001>, 2019.
- Juliussen, H. and Humlum, O.: Thermal regime of openwork block fields on the mountains Elgåhogna and Sølen, central-eastern Norway, *Permafrost and Periglacial Processes*, 19, 1–18, <https://doi.org/10.1002/ppp.607>, 2008.
- 660 Kääb, A., Frauenfelder, R., and Roer, I.: On the response of rockglacier creep to surface temperature increase, *Global and Planetary Change*, 56, 172–187, <https://doi.org/10.1016/j.gloplacha.2006.07.005>, 2007.
- Langer, M., Westermann, S., Boike, J., Kirillin, G., Grosse, G., Peng, S., and Krinner, G.: Rapid degradation of permafrost underneath waterbodies in tundra landscapes—toward a representation of thermokarst in land surface models, *Journal of Geophysical Research: Earth Surface*, 121, 2446–2470, <https://doi.org/10.1002/2016JF003956>, 2016.
- 665 Liestøl, O.: Lokalt omrøde med permafrost i Gudbrandsdalen, *Norsk Polarinstitutt Aarbok*, 1965, 129–133, 1966
- Lilleøren, K. S. and Etzelmüller, B.: A regional inventory of rock glaciers and ice-cored moraines in Norway, *Geografiska Annaler: Series A, Physical Geography*, 93, 175–191, <https://doi.org/10.1111/j.1468-0459.2011.00430.x>, 2011.
- Lilleøren, K. S., Etzelmüller, B., Rouyet, L., Eiken, T., and Hilbich, C.: Transitional rock glaciers at sea-level in Northern Norway, *Earth Surface Dynamics Discussions*, pp. 1–29, <https://doi.org/10.5194/esurf-2022-6>, 2022.
- 670 Liston, G. E. and Sturm, M.: A snow-transport model for complex terrain, *Journal of Glaciology*, 44, 498–516, <https://doi.org/10.3189/S0022143000002021>, 1998.
- Mamot, P., Weber, S., Eppinger, S., and Krautblatter, M.: A temperature-dependent mechanical model to assess the stability of degrading permafrost rock slopes, *Earth Surface Dynamics*, 9, 1125–1151, <https://doi.org/10.5194/esurf-9-1125-2021>, 2021.



- 675 Martin, L. C. P., Nitzbon, J., Aas, K. S., Etzelmüller, B., Kristiansen, H., and Westermann, S.: Stability conditions of peat plateaus and palsas in northern Norway, *Journal of Geophysical Research: Earth Surface*, 124, 705–719, <https://doi.org/10.1029/2018JF004945>, 2019.
- Monnier, S. and Kinnard, C.: Interrogating the time and processes of development of the Las Liebres rock glacier, central Chilean Andes, using a numerical flow model, *Earth Surface Processes and Landforms*, 41, 1884–1893, <https://doi.org/10.1002/esp.3956>, 2016.
- 680 Nelson, F. E., Anisimov, O. A., and Shiklomanov, N. I.: Subsidence risk from thawing permafrost, *Nature*, 410, 889–890, <https://doi.org/10.1038/35073746>, 2001.
- Nesje, A., Matthews, J. A., Linge, H., Bredal, M., Wilson, P., and Winkler, S.: New evidence for active talus-foot rock glaciers at Øyberget, southern Norway, and their development during the Holocene, *The Holocene*, 31, 1786–1796, <https://doi.org/10.1177/09596836211033226>, 2021.
- 685 Obu, J., Westermann, S., Bartsch, A., Berdnikov, N., Christiansen, H. H., Dashtseren, A., Delaloye, R., Elberling, B., Etzelmüller, B., Kholodov, A., et al.: Northern Hemisphere permafrost map based on TTOP modelling for 2000–2016 at 1 km² scale, *Earth-Science Reviews*, 193, 299–316, <https://doi.org/10.1016/j.earscirev.2019.04.023>, 2019.
- Painter, S. L. and Karra, S.: Constitutive model for unfrozen water content in subfreezing unsaturated soils, *Vadose Zone Journal*, 13, <https://doi.org/10.2136/vzj2013.04.0071>, 2014.
- 690 Porter, C., Morin, P., Howat, I., Noh, M., Bates, B., Peterman, K., Keeseey, S., Schlenk, M., Gardiner, J., Tomko, K., et al.: ArcticDEM, Harvard Dataverse [data set], V1, <https://doi.org/10.7910/DVN/OHHUKH>, 2018.
- Renette, C.: Parameter files and code for simulations in "Simulating the effect of subsurface drainage on the thermal regime and ground ice in blocky terrain, Norway" [Data set], Zenodo, <https://doi.org/10.5281/zenodo.6563651>, 2022.
- 695 Romundset, A., Bondevik, S., and Bennike, O.: Postglacial uplift and relative sea level changes in Finnmark, northern Norway, *Quat. Sci. Rev.*, 30, 2398–2421, <https://doi.org/10.1016/j.quascirev.2011.06.007>, 2011.
- Sæmundsson, Þ., Morino, C., Helgason, J. K., Conway, S. J., and Pétursson, H. G.: The triggering factors of the Móafellshyrna debris slide in northern Iceland: Intense precipitation, earthquake activity and thawing of mountain permafrost, *Science of the total environment*, 621, 1163–1175, <https://doi.org/10.1016/j.scitotenv.2017.10.111>, 2018.
- 700 Saloranta, T.: Simulating snow maps for Norway: description and statistical evaluation of the seNorge snow model, *The Cryosphere*, 6, 1323–1337, <https://doi.org/10.5194/tc-6-1323-2012>, 2012.
- van Everdingen, R. O.: Multi-language glossary of permafrost and related ground-ice terms, International Permafrost Association, 1998.
- Vionnet, V., Brun, E., Morin, S., Boone, A., Faroux, S., Le Moigne, P., Martin, E., and Willemet, J.-M.: The detailed snowpack scheme Crocus and its implementation in SURFEX v7. 2, *Geoscientific Model Development*, 5, 773–791, <https://doi.org/10.5194/gmd-5-773-2012>, 2012.
- Westermann, S., Schuler, T., Gislås, K., and Etzelmüller, B.: Transient thermal modeling of permafrost conditions in Southern Norway, *The Cryosphere*, 7, 719–739, <https://doi.org/10.5194/tc-7-719-2013>, 2013.



- 710 Westermann, S., Langer, M., Boike, J., Heikenfeld, M., Peter, M., Etzelmüller, B., and Krinner, G.: Simulating the thermal regime and thaw processes of ice-rich permafrost ground with the land-surface model CryoGrid 3, *Geoscientific Model Development*, 9, 523–546, <https://doi.org/10.5194/gmd-9-523-2016>, 2016.
- 715 Westermann, S., Ingeman-Nielsen, T., Scheer, J., Aalstad, K., Aga, J., Chaudhary, N., Etzelmüller, B., Filhol, S., Kääb, A., Renette, C., Schmidt, L. S., Schuler, T. V., Zweigel, R. B., Martin, L., Morard, S., Ben-Asher, M., Angelopoulos, M., Boike, J., Groenke, B., Miesner, F., Nitzbon, J., Overduin, P., Stuenzi, S. M., and Langer, M.: The CryoGrid community model (version 1.0) – a multi-physics toolbox for climate-driven simulations in the terrestrial cryosphere, *Geosci. Model Dev. Discuss.* [preprint], <https://doi.org/10.5194/gmd-2022-127>, in review, 2022.
- Wicky, J. and Hauck, C.: Numerical modelling of convective heat transport by air flow in permafrost talus slopes, *The Cryosphere*, 11, 1311–1325, <https://doi.org/10.5194/tc-11-1311-2017>, 2017.
- 720 Zweigel, R., Westermann, S., Nitzbon, J., Langer, M., Boike, J., Etzelmüller, B., and Vikhamar Schuler, T.: Simulating snow redistribution and its effect on ground surface temperature at a high-Arctic site on Svalbard, *Journal of Geophysical Research: Earth Surface*, 126, e2020JF005673, <https://doi.org/10.1029/2020JF005673>, 2021.